

## Original Article

# Proteomic screening identifies PML/p53 axis as a potential treatment target of facial nerve schwannomas

Zhigang Wang<sup>1,2,3\*</sup>, Hongsai Chen<sup>1,2,3\*</sup>, Lu Xue<sup>1,2,3</sup>, Weiwei He<sup>1,2,3</sup>, Lianying Jiang<sup>4</sup>, Zhaoyan Wang<sup>1,2,3</sup>, Hao Wu<sup>1,2,3</sup>

<sup>1</sup>Department of Otolaryngology Head & Neck Surgery, The Ninth People's Hospital, Shanghai Jiao Tong University School of Medicine, Shanghai, China; <sup>2</sup>Ear Institute, School of Medicine, Shanghai Jiao Tong University, Shanghai, China; <sup>3</sup>Shanghai Key Laboratory of Translational Medicine on Ear and Nose Diseases, Shanghai, China; <sup>4</sup>Department of Neurology, The People's Hospital of Shanghai Pudong New Area Affiliated to Shanghai University of Medicine and Health Sciences, Shanghai, China. \*Equal contributors.

Received February 10, 2020; Accepted July 4, 2020; Epub August 15, 2020; Published August 30, 2020

**Abstract:** Facial nerve schwannomas (FNS) represents one of the more difficult treatment paradigms in neurotology. The aim of this study is to investigate the molecular alterations of FNS, thus providing potential targets treatable in the tumour. We for the first time suggest that the deficiency of merlin (the product of *NF2* tumour suppressor) is probably one of the key mechanisms underlying FNS tumorigenesis, although no disease-causing *NF2* mutations were demonstrated in tumour samples. TMT-labeled spectrometry analysis was used to identify the proteome of FNS relative to nerve controls. Eighty-four significantly deregulated proteins were identified, among which the PML tumour suppressor showed the most significantly increased expression. The PML protein was distributed in the nucleoplasm of non-tumorous Schwann cells, whereas it was preferentially confined to the cytoplasm of FNS cultures. Overexpression of PML and p53, partner proteins positively regulating each other to trigger apoptosis, was further confirmed in FNS tissues/cultures, and this correlated with a significant decrease in the proliferation of FNS cultures in comparison to Schwann cells. It is therefore probable that PML-p53 overexpression may occur as part of protective cellular mechanisms in response to the proliferation signal mediated by loss of merlin in FNS, in accordance with the fact that the tumour is benign slow-growing. This hypothesis was supported by the finding that the p53 activator nutlin-3 could exert dose-dependent inhibitory effects on FNS cultures via a cooperative induction of PML-p53 levels. Thus, the current study may present a potential treatment target directed on the molecular mechanisms of this disease.

**Keywords:** Facial nerve schwannomas, mutation, proteomics, apoptosis, treatment

## Introduction

Facial nerve schwannomas (FNS) are benign neoplasms arising from the Schwann cells that ensheath the facial nerve (cranial nerve VII) at any point along the nerve and patients most commonly present with facial paresis and/or hearing loss. In clinical practice, FNS are rarer than their vestibular nerve (cranial nerve VIII, the most common site for the occurrence of schwannoma) counterparts [1]. Similar to vestibular schwannomas (VSs), FNS typically grow slowly over time. Sporadic FNS represent almost all cases; the tumour sometimes occurs as part of two hereditary cancer syndromes - neurofibromatosis type 2 [2] and schwannomatosis [3].

Although a paucity of genetic studies specific to FNS exists, multiple genetic studies of VSs, mixed types of schwannomas and schwannomatosis have been conducted. Loss-of-function mutations of the *NF2* gene on chromosome 22q is associated with the development of both sporadic and neurofibromatosis type 2-related schwannoma [4, 5]. Genes other than the *NF2* gene are responsible for the development of schwannomatosis-related schwannomas [6]; these patients harbor concomitant mutational inactivation of *SMARCB1* or *LZTR1*, both of which are also located on chromosome 22q. In a study comprising 17 sporadic schwannomas [7], including 13 VSs, 3 cervical schwannomas, and 1 FNS, 82% of the tumours had at least one *NF2* point mutation; interestingly, this FNS sam-

ple had no such mutation, but showed loss of 22q arm instead. The *NF2* gene product merlin is a multi-suppressor present in the cell membrane and nucleus [8]. Mutation in the *NF2* gene, leading to loss of merlin protein, causes abnormal proliferation of schwannoma/Schwann cells [9, 10].

Surgical treatment of FNS is challenging because the risk of facial nerve injury is high. There is a clear need to identify potential targets that are active and treatable in the tumour. Mass spectrometry (MS) has emerged as a comprehensive and versatile tool for in-depth characterization of the protein components of biological systems. The use of MS-based proteomics to screen for proteins that may act as drug targets has been reported in primary human tumour cells of schwannomas and meningiomas [11]. To our knowledge, the molecular biology of FNS remains largely unknown. Here, we report our mutational analysis of three schwannoma susceptibility genes (*NF2*, *SMARCB1*, and *LZTR1*) among twelve sporadic FNS, focusing on the proteomic identification of differentially-expressed proteins in the tumour, thus providing insights into the pathogenesis of this disease.

### Materials and methods

#### *Tumour samples*

In this study, we analyzed twelve FNS obtained during surgical operations in our department. Clinical diagnosis of FNS was established on the basis of history, physical examination, characteristic imaging features, and operative findings. All of the cases were sporadic with no family history. Four vestibular schwannomas were included as positive controls of mutation analyses. All tumours were subjected to histological examinations to confirm the diagnosis of schwannomas. The tumours were either kept at  $-80^{\circ}\text{C}$  until DNA/protein extraction or collected immediately for primary culture after resection. Three great auricular nerves (GANs) obtained during parotidectomy were included as non-tumoral controls. Informed written consent was obtained from all patients donating tissue. This study was approved by the Institutional Review Board of the ethics committee of The Ninth People's Hospital affiliated to School of Medicine, Shanghai Jiao Tong University.

#### *Direct sequencing analysis*

Sanger sequencing was conducted to detect point mutations or small deletions/insertions in the genes. DNA extraction from the tumour specimens was performed using the TIANamp Genomic DNA Kit (Tiangen Biotech, Beijing, China). The whole coding sequence and exon-intron boundaries of the genes were amplified by the polymerase chain reaction (PCR) using standard methods and underwent bidirectional sequencing. The sequence data were analyzed using the Sequencer 4.9 software (Genecode, MI, USA) and compared with the sequences of *NF2* (NM\_016418), *LZTR1* (NM\_006767.3) and *SMARCB1* (NM\_003073.3) in GeneBank. Mutations were described according to the standard nomenclature for DNA sequence changes reported by the Human Genome Variation Society (HVGs).

#### *Tandem mass tag (TMT) labeling quantitative proteomic*

In brief, tumour tissues were lysed, digested, and TMT labeled according to the manufacturer's protocol. TMT-labeled peptides were separated and analyzed with a nano-UPLC (EASY-nLC1200) coupled to Q-Exactive mass spectrometry (Thermo Finnigan). Separation was performed using a reversed-phase column (Acclaim PepMap RSLC, Thermo Scientific). Mobile phase A consisted of 0.1% formic acid and 2% acetonitrile. Mobile phase B consisted 80% acetonitrile and 0.1% formic acid. Mass spectrometry (MS) was performed in a data-dependent mode with single full-scan mass spectrum in the orbitrap ( $m/z$  350-1600, 70000 resolution), and MS/MS scans were carried out in data-dependent mode at 32 per cent collision energy.

The resulting MS/MS data were processed using MaxQuant with an integrated Andromeda search engine (V.1.5.6.0). The protein sequence database (Uniprot\_organism\_2016\_09) was downloaded from UNIPROT. This database and its reverse decoy were then searched against by MaxQuant software. Trypsin was set as specific enzyme with up to 3 miss cleavage; Oxidation [M] and acetyl [protein N-term] were considered as variable modification (max number of modifications per peptide is 3), and carbamidomethyl [C] was set as fixed modification; False discovery rate (FDR) thresholds for pro-

## Proteomic profiling of facial nerve schwannomas

teins, peptides and modification sites were specified at 1%. Only unmodified unique peptides were used for quantification. For quantification analysis, proteins were quantified by normalized summed peptide intensities. Proteins were considered to be significantly differentially expressed if the TMT ratios were  $>1.5$  or  $<0.67$  in tumour samples compared to those in nerve controls, with a  $P$  value  $<0.05$ , which was statistically analyzed by a paired  $t$ -test.

### *Protein-protein interaction (PPI) and functional enrichment analysis*

The STRING (Search Tool for the Retrieval of Interacting Genes/Proteins) is a curated knowledge database and used for illustration of predicted interactions of identified proteins and neighbor genes. The proteins expressed significantly differentially in tumours relative to controls were processed in STRING v11.0 (<https://string-db.org/>) to obtain high-confidence interaction data (score  $\geq 0.7$ ). The PPI network was visualized using the Cytoscape 3.2.1 software (<https://cytoscape.org/>). The Kyoto Encyclopedia of Genes and Genomes (KEGG) database is used to annotate the protein pathways. The gene ontology (GO) analysis, including biological process (BP), cellular component (CC), and molecular function (MF), helps identify the biological traits for proteomics data. To annotate the proteins at the functional level, KEGG pathways and GO terms were analyzed with the DAVID database (<https://david.ncifcrf.gov/>). Statistically significant  $P$  values were set at 0.05 or less.

### *Western blotting*

Tumour tissues or cells were ultrasonicated in Lysis Buffer (Beyotime, Shanghai China) containing 1 mM phenylmethanesulfonyl fluoride. Tissue/cell extract samples were subjected to Western blotting with anti-PML (#ab179466, Abcam), anti-CD44 (#ab189524, Abcam), anti-merlin (#HPA003097, Sigma-Aldrich), anti-p53 (#P6874, Sigma-Aldrich) and anti- $\beta$ -actin (#A1-978, Sigma-Aldrich) antibodies. The blots were detected using a chemiluminescence HRP substrate (Millipore). The intensities of the bands on blots were analyzed using Imager Lab Software (Bio-Rad).

### *Immunohistochemistry*

Four-micrometer-thick sections were cut for immunohistochemical studies, which were per-

formed using standard techniques, heat induced epitope retrieval buffer, and primary antibodies against Ki-67 (Abcam; #ab189524) and cleaved-Caspase 3 (Cell Signaling; #9664) at 4°C overnight. On the following day, biotinylated secondary antibodies were applied, followed by the addition of streptavidin-peroxidase conjugate. After visualization with DAB, the tissue sections were briefly counterstained with hematoxylin.

### *Cell culture and immunofluorescence*

Human Schwann cells (HSC) were purchased from ScienCell Research Laboratories (Cat. No. 1700; Carlsbad, CA, USA), and cultured in Schwann Cell Medium (ScienCell, Cat. No.1701). The primary culture of FNS was performed according to protocols previously described [12]. Briefly, tumour tissues were cut into 1 mm<sup>3</sup> segments, washed with phosphate-buffered saline, and then incubated in media with enzyme mixture containing 250 U/mL Hyaluronidase Type I-S (Sigma-Aldrich, MO, #C1639) and 160 U/mL Collagenase Type I (Sigma-Aldrich, MO, #3506) in DMEM/F12 medium for 18 h at 37°C. After the enzymatic incubation of the culture, the cells were re-suspended in Schwann Cell Medium, passed through a 200 mesh filter screen, and finally transferred to 6-cm culture dishes pre-coated with poly-Lornithine and laminin (BD Biosciences, MA, #35-4232). For immunofluorescence, cells on glass slides were fixed with 4% paraformaldehyde, permeabilized in 0.3% Triton X-100, and then blocked with bovine serum albumin before the incubation with anti-PML (#ab179466, Abcam), anti-p53 (#P6874, Sigma-Aldrich) antibodies and Alexa Fluor® 488 Phalloidin (#A12379, Thermo) used for F-actin cytoskeleton. Alexa-488- and Alexa-555-conjugated goat anti-mouse and goat anti-rabbit antibodies were used as secondary antibodies. The sections were nuclear counterstained with 4, 6-Diamidino-2-phenylindole (DAPI, #1985274, Thermo). Images were acquired using a confocal microscope (LSM 880; Carl Zeiss GmbH, Germany).

### *Cell viability and EdU incorporation assays*

Nutlin-3 (#S1778, Beyotime) was dissolved in DMSO at a concentration of 20 mg/mL until use. The effect of the drug on cell viability was determined by a Cell Counting Kit-8 (CCK-8; Dojindo Laboratories, Kumamoto, Japan). Briefly, cells were grown to 50% confluency in

## Proteomic profiling of facial nerve schwannomas

96-well plates before the incubation with different concentrations of Nutlin-3. At each specified time point, 10  $\mu$ l/well CCK-8 solutions were added and cells were incubated for an additional 1 h at 37°C. The absorbance of each well was analyzed at 450 nm using a SpectraMax-190 microplate reader (Molecular, USA). The DNA synthesis activity of cells was assessed by the 5-ethynyl-20-deoxyuridine (EdU, Guangzhou RiboBio Co., Ltd.) labeling as previously described [13]. Images were captured under LAS AF software V4.3 (Leica Microsystems, Inc., Buffalo Grove, IL, USA). DAPI staining was used to determine the total cell number within each field of view. Quantification of EdU incorporating-cells was calculated as follows: EdU-positive cell numbers/total numbers  $\times$ 100%.

### *Statistical analysis*

Statistical analyses were performed using the SPSS statistics software (SPSS, Chicago, IL). Data were expressed as mean  $\pm$  standard deviation (SD) from at least three independent experiments. The between-group differences were assessed using one-way analysis of variance (ANOVA) or Student's *t*-test.  $P < 0.05$  was considered statistically significant.

## Results

### *Mutational analyses reveal no significant disease-causing mutations in FNS*

Mutational analysis revealed that 5 of 12 FNS harbored at least one silent (alias synonymous) mutation within *LZTR1* or *SMARCB1*. The variations c.210G>A and c.1683C>T in *LZTR1* occurred more frequently. However, DNA analysis for *NF2* yielded negative results in all these specimens (Table S1). These synonymous variations were not likely to be disease-causing mutations because they did not affect the amino acid sequence of the resulting protein. In their vestibular counterparts as controls, two patients, T554 and T563, were identified with a truncating mutation that resulted in an abnormal protein. Additionally, the vestibular schwannoma T561 also had a synonymous mutation c.210G>A in *LZTR1*, suggesting these variations were not specific to FNS.

### *Proteomics analysis of FNS compared with normal nerve controls*

Using tandem mass tag protein labeling analysis, 84 proteins were significantly and differen-

tially expressed in FNS compared with normal nerves (Table S2). Among these proteins, 38 and 46 proteins were found to be up- and down-regulated, respectively (Figure 1A). The top 10 proteins up-regulated or down-regulated in FNS were shown in Table 1. PMP2, the peripheral myelin protein, was the most highly down-regulated protein. However, this protein was found to be overexpressed in dermal and vestibular schwannomas [14, 15]. A possible explanation for the conflicting results is the variable expression patterns of PMP2 in schwannomas of different nerve origin. The promyelocytic leukemia (PML) protein showed the most significantly increased expression. PML, a tumour suppressor implicated in apoptosis, was initially discovered in patients with acute promyelocytic leukemia [16]. Since then, its importance has been emerging far beyond leukemia, to an extensive range of neoplasms, including solid tumours [17]. Koken and colleagues [18] observed a gradual increase in PML expression from benign dysplasia to carcinoma. When the malignant cells turned invasive, they lost PML expression. Another interesting observation came from Zhu and colleagues [19], who reported the up-regulation of PML in nuclear receptor tailless (Tlx)-mutant brain tumours that are very small and benign, suggesting a general inhibition of tumour growth after Tlx inactivation. These findings are consistent with the functions of PML as a tumour suppressor or a pro-apoptotic factor. The suppression of apoptosis is generally considered the focal mechanism of tumorigenesis and, in other words, increased apoptosis presumably results in slow tumour growth. Therefore, PML overexpression may contribute to anti-tumour activity in FNS, leading to the tumor being benign and slow-growing.

A protein interaction network was generated using the STRING database to identify potential binding partners for host-specific biomarkers (Figure 1B). A protein-protein interaction 'hot spot' was shown in CD44 with its neighbors (PML, CD9, CD34, LAMA2, LAMB1, ALDH1A1, ITGAV, GBA, RDX, DCN, and NID1). CD44 was identified as one of the top most significantly increased proteins in FNS; the protein plays a key role in Schwann cell-neuron interactions and shows increased expression in vestibular schwannomas [20]. Additionally, the ribosomal proteins RPL28, RPL3, RPS28, RPS3, and RPS9 and the amyotrophic lateral sclerosis-



# Proteomic profiling of facial nerve schwannomas

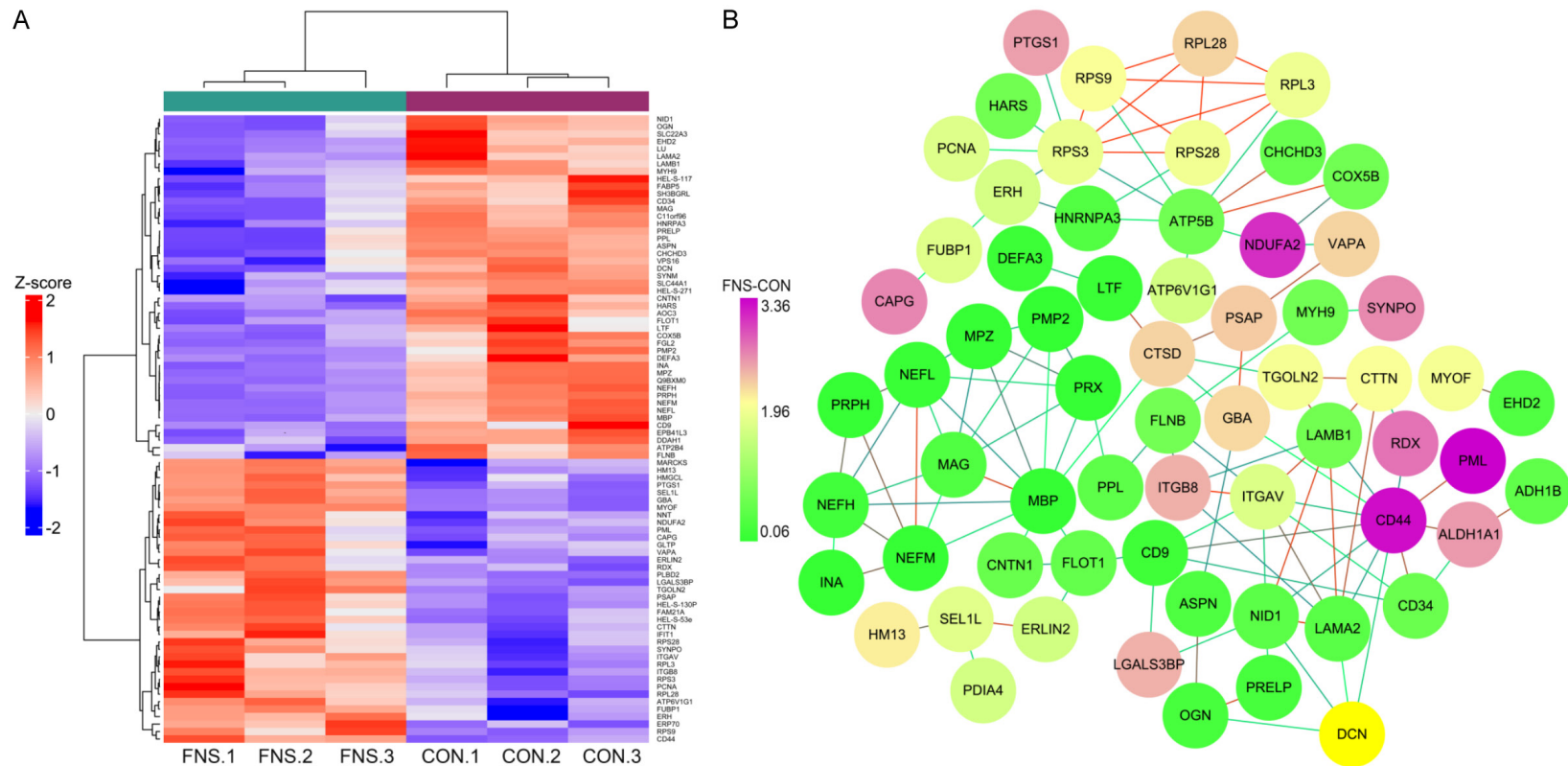


**Figure 1.** Proteomic analysis of differentially expressed proteins between FNS and nerve controls (CON). A. Hierarchically clustered heat maps of the 84 significantly deregulated proteins in 3 samples from each group. Among these proteins, 38 and 46 proteins were found to be up- and down-regulated, respectively. PML showed the most significantly increased expression. Red represents a high z-score, and blue represents a low z-score; the “row names” FNS.1-3 indicate tumours T333, T558 and T585. B. Protein-protein interaction (PPI) network of the above deregulated proteins. A protein-protein interaction ‘hot spot’ was shown in CD44 with its neighbors. Circular nodes denote proteins and their connecting edges denote protein-protein interactions. The node size is made proportional to the fold-change of the corresponding modulated protein.

## Proteomic profiling of facial nerve schwannomas

**Table 1.** The top 10 proteins up-regulated or down-regulated in FNS compared with nerve control

Gene_symbol	Protein_name	Fold changes
PML	promyelocytic leukemia	3.36
CD44	CD44 molecule	3.29
NDUFA2	NADH dehydrogenase (ubiquinone) 1 alpha subcomplex, 2	3.11
RDX	radixin	2.72
CAPG	capping protein (actin filament), gelsolin-like	2.61
SYNPO	synaptopodin	2.6
ALDH1A1	aldehyde dehydrogenase 1 family, member A1	2.51
PTGS1	prostaglandin-endoperoxide synthase 1	2.48
FAM21A	family with sequence similarity 21, member A	2.44
ITGB8	integrin, beta 8	2.38
PMP2	peripheral myelin protein 2	0.05
EPB41L3	erythrocyte membrane protein band 4.1-like 3	0.06
FGL2	fibrinogen-like 2	0.06
MBP	myelin basic protein	0.07
INA	internexin neuronal intermediate filament protein, alpha	0.08
MPZ	myelin protein zero	0.08
PRPH	peripherin	0.09
NEFM	neurofilament	0.08
PRX	periaxin	0.08
LTF	lactotransferrin	0.11

related proteins NEFH, NEFL, NEFM, and PRPH formed a prominent tightly connected protein network. The differentially expressed proteins were then subjected to Gene Ontology (GO) analysis (**Figure 2A-C**) and were categorized into three GO groups-biological processes (BP), cellular components (CC), and molecular functions (MF). Up-regulated proteins were significantly involved in GO terms such as cellular process, cytoplasm, and peptide/protein binding, while down-regulated proteins were associated with GO terms such as cellular process, intracellular organelle and amide binding (**Table S3**). When KEGG analysis was performed (**Figure 2D**), the most frequently enriched pathways were found to be associated with the extracellular matrix-receptor interaction (CD44, ITGAV, ITGB8, LAMA2, and LAMB1) and cell adhesion (CD34, CNTN1, ITGAV, ITGB8, MAG, and MPZ), both of which have been predicted to play important roles in schwannoma biology [21, 22].

### Western blotting analysis of merlin, CD44 and PML-p53 partners

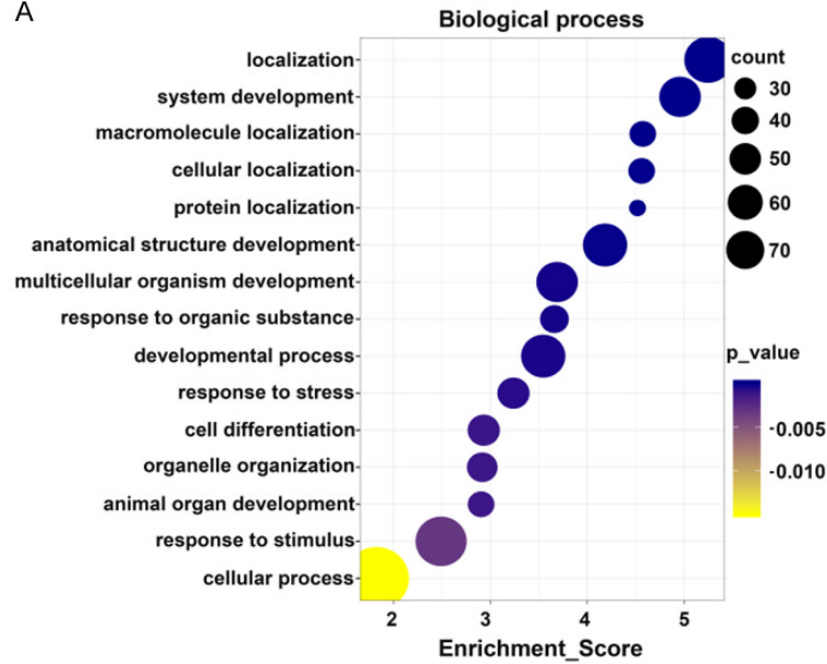
Western blotting serves as a more specific and efficient method of validation, when targets are narrowed down to individual functionally rele-

vant proteins. Next, we used the method to confirm our proteomic findings of two significant candidates (PML and CD44) along with proteins of interest, including the *NF2* product merlin (**Figure 3**). The blots showed significantly increased levels of CD44 (4.9-fold) and PML (18.2-fold) in FNS relative to nerve controls, confirming their differential expression patterns determined in proteomic analysis. Although there was a considerable amount of merlin in nerve controls, zero or very low levels of the protein were observed in FNS samples. However, no detectable mutations were observed in the *NF2* gene associated with merlin deficiency, in any of these tumours. One possible explanation is that the tumours may have harbored undetected mutations in the *NF2* gene. Similar observations were found in vestibular schwannomas in which merlin loss frequently occurred without *NF2* mutations [23]. The deficiency in merlin protein coincided with CD44 up-regulation in FNS (**Figure 3**), further confirming a previous report indicating that merlin depletion was associated with an increased CD44 expression in Schwann cells [10].

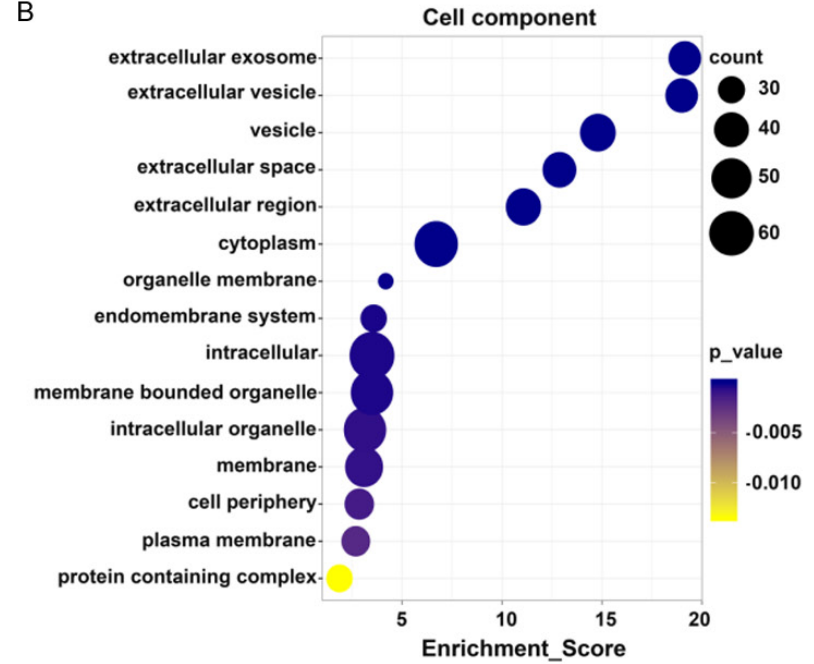
A critical anti-cancer function of PML is to facilitate the stabilization of the key tumour suppressor p53 [24]. PML is also a transcriptional

Proteomic profiling of facial nerve schwannomas

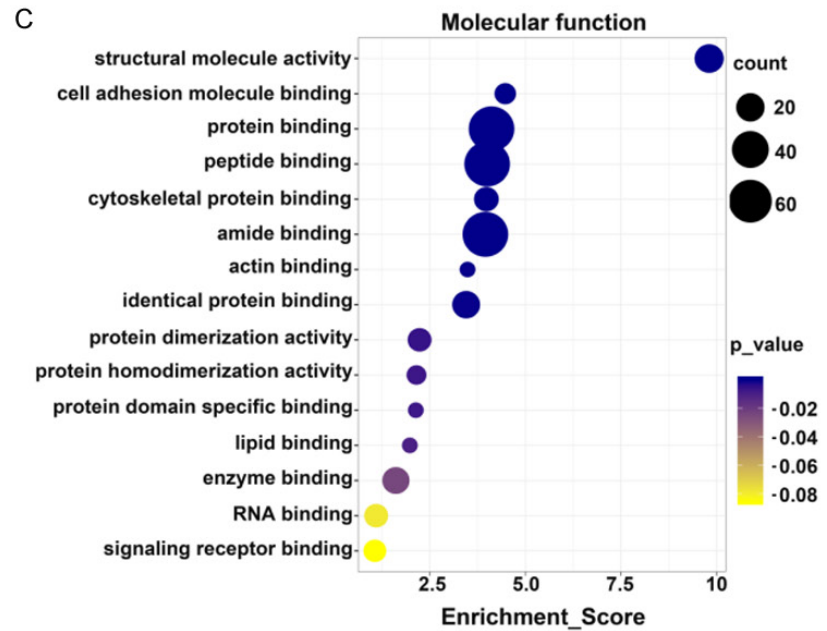
A



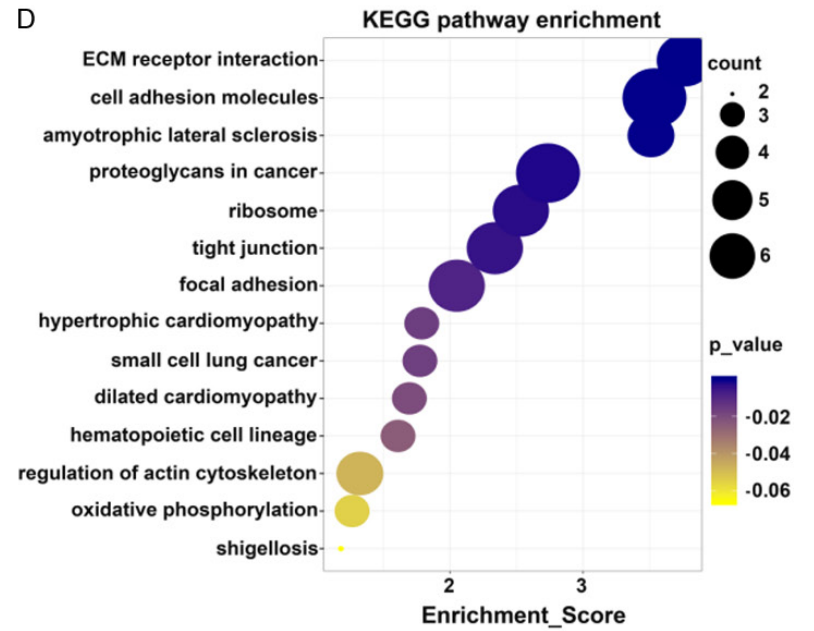
B



C



D



## Proteomic profiling of facial nerve schwannomas

**Figure 2.** Enrichment analysis of GO terms and KEGG pathways. (A-C) The GO terms in the biological process (A), cellular component (B) and molecular function (C) categories are depicted. Up-regulated proteins were significantly involved in GO terms such as cellular process, cytoplasm, and peptide/protein binding, while down-regulated proteins were associated with GO terms such as cellular process, intracellular organelle and amide binding. (D) KEGG analysis showed that the most frequently enriched pathways were associated with extracellular matrix-receptor interaction and cell adhesion. The color of each dot denotes the *P* value, and the size of each dot denotes the number of proteins involved in each pathway.

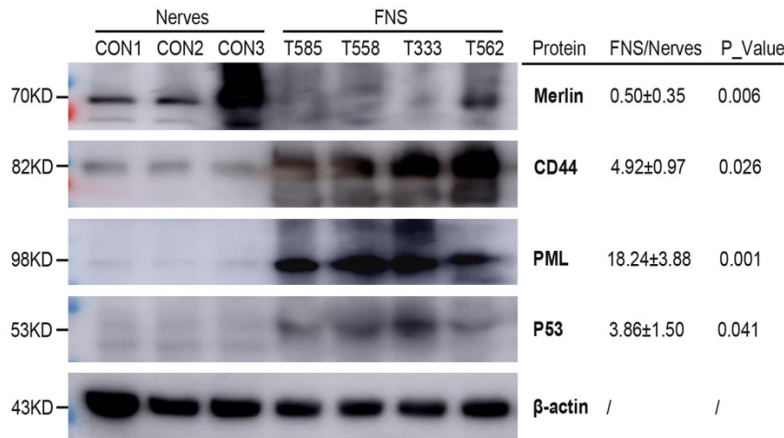


**Figure 3.** The expression of PML, CD44, merlin and p53 in FNS compared with nerve controls by Western Blotting. The left panel shows representative Western blot bands of the four target proteins for each group. The blots showed significantly increased levels of CD44 (4.9-fold) and PML (18.2-fold) in FNS relative to nerve controls, confirming their differential expression patterns determined in proteomic analysis. P53, a partner protein of PML, was found to be overexpressed in FNS samples. Zero or very low levels of the protein were observed in the tumours. The band intensities of proteins in each group are normalized to  $\beta$ -actin to obtain a gray scale value. The average gray scale values of target proteins in FNS group are expressed relative to those in the nerve control group to obtain relative average gray scale values, which were listed in the right panel. Data are presented as the mean  $\pm$  SD. \* $P < 0.05$ ; \*\* $P < 0.01$  compared with controls. Full-length gels are presented in [Figure S1](#).

target of p53 [25], implying that the two tumour suppressors regulate each other through a positive regulatory loop. The partner proteins, PML and p53, have been reported to be overexpressed in gallbladder carcinoma [26]. We showed that both proteins were up-regulated in FNS relative to nerve controls (**Figure 3**). This finding agreed with the changes in protein expression observed in FNS cultures (FSC) compared with human Schwann cells (HSC) (**Figure 4A**). PML displays tumor suppression functions by acting both in the cytoplasm and nucleus [27]. In normal cells, PML is enriched in discrete nuclear substructures known as PML-nuclear bodies (PML-NBs), which form a speckled pattern [28]. In HSC, as expected, PML exhibited a speckled pattern of distribution in the nucleoplasm. Interestingly, FSC displayed an altered PML-staining pattern; the pro-

tein was preferentially confined to the cytoplasm of tumour cells (**Figure 4B**).

### *Overexpression of PML and p53 is associated with the benign behavior of FNS*

Tumourigenesis reflects a loss of balance between cell proliferation and cell death. The occurrence of apoptosis in schwannomas has already been reported by several studies [29-31]. An earlier proteomic study [32] on vestibular schwannomas has shown increased expression of four proteins (Annexin V, Annexin A4, Annexin A2, and YWHAZ) that are likely to accelerate apoptosis. Similar to PML, p53 tumour suppressor plays an important role in the induction of apoptosis and cellular senescence. An elevated p53 level was previously

demonstrated to induce senescence in benign meningiomas and to protect against recurrence [33]. The observation that the apoptotic markers PML and p53 were up-regulated in FNS was supported by the fact that FNS are benign, slow-growing tumours. The proliferation of FSC was investigated using the 5-ethynyl-2'-deoxyuridine (EdU) incorporation assay. Consistent with the nature of FNS, the percentage of EdU-positive cells was significantly lower ( $8.2 \pm 2.3\%$  vs.  $58.9 \pm 13.2\%$ ;  $P = 0.003$ ) in FSC than in HSC (**Figure 4C, 4D**).

Immunohistochemistry staining of Ki-67 and Cleaved caspase-3 may provide information on cell death or cell proliferation in FNS. The Ki-67 nuclear antigen is associated with cell proliferation. Cleaved caspase-3 detects endogenous levels of the large fragment of activated caspase-3, a protease that mediates apoptosis. As



## Proteomic profiling of facial nerve schwannomas

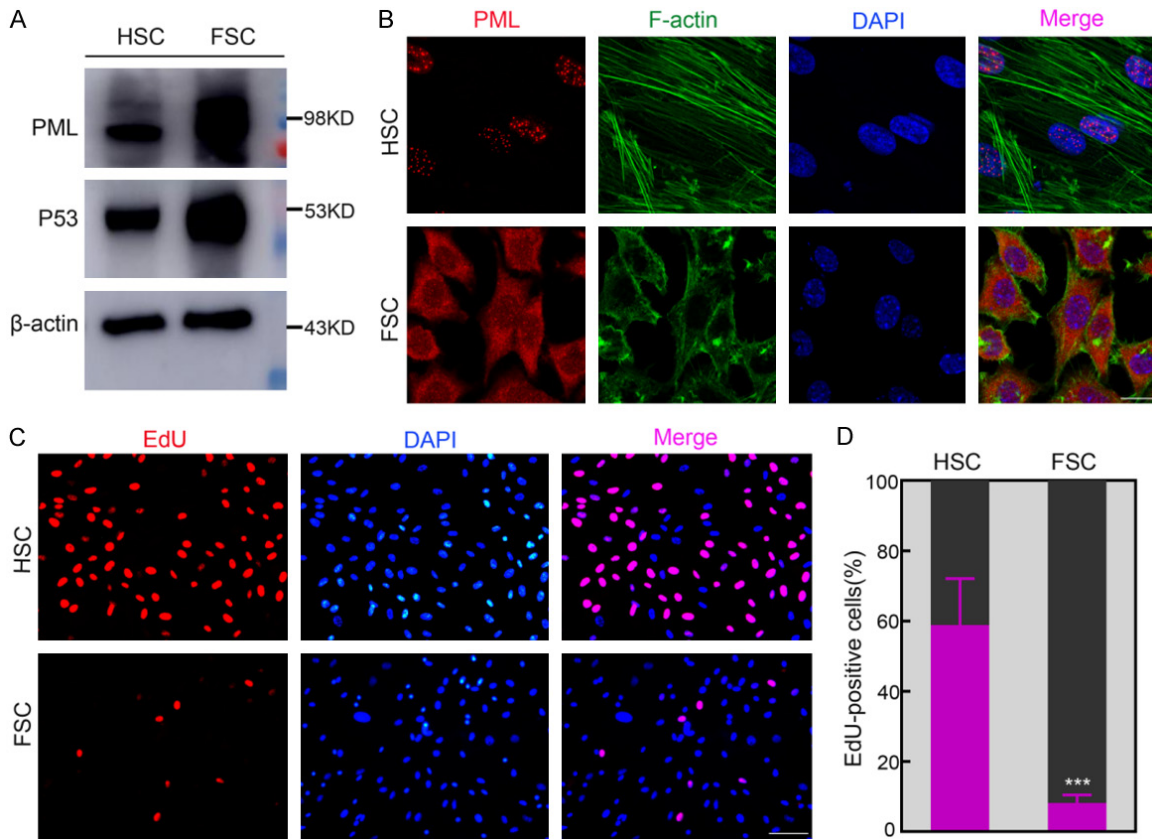


**Figure 4.** Comparison of PML/p53 expression and proliferation between primary facial nerve schwannoma cells (FSC) and Human Schwann cells (HSC). **A.** Western Blotting demonstrated that both PML and p53 proteins were up-regulated in FSC compared with HSC. **B.** PML showed a speckled pattern of distribution in the nucleoplasm of HSC by immunofluorescent staining. PML was preferentially confined to the cytoplasm of FSC. Scale bar =25  $\mu$ m. **C.** The proliferation of FSC compared with HSC was investigated using the 5-ethynyl-2'-deoxyuridine (EdU) incorporation assay. Representative images of EdU labelling and DAPI staining were shown. **D.** The percentage of EdU-positive cells was significantly lower ( $8.2 \pm 2.3\%$  vs.  $58.9 \pm 13.2\%$ ;  $P=0.003$ ) in FSC than in HSC. Quantification of EdU incorporating-cells is calculated as follows: EdU-positive cell numbers (red dots)/total numbers (blue dots)  $\times 100\%$ . Scale bar =100  $\mu$ m. At least 3 random images are taken from each well. Data are represented as mean  $\pm$  SD. \*\* $P < 0.01$  compared with controls. Full-length gels are presented in [Figure S2](#).

shown in **Figure 5**, significantly higher expression of cleaved-Caspase 3 was noted in FNS than the nerve control. Furthermore, no significant expression of Ki-67 was detected in both tumors and nerve control. The increase in the expression of cleaved-Caspase 3 was associated the regulation of apoptosis by PML and p53 in FNS, and was therefore consistent with the benign behavior of FNS.

### *Coordinated induction of the PML-p53 level inhibits the proliferation of FNS cultures (FSC)*

Because PML and p53 regulate each other through a positive regulatory loop, further induction of p53 and PML levels may inhibit the growth of FNS. One of the most promising p53

activating agents is nutlin-3, which binds to the p53 inhibitor Mdm2, leading to the stabilization of p53 protein. Nutlin-3 is selective for p53 because the agent induces cell cycle arrest in wild-type cells, but not p53-null cells [34]. Recent studies have demonstrated that nutlin-3, used alone or in combination with other drugs, can effectively block the proliferation of primary cultures from vestibular schwannomas through p53 reactivation [23]. Next, we asked whether the induction of p53 by nutlin-3 inhibited the proliferation of FNS cultures, and specifically, whether this drug will trigger p53-mediated up-regulation of PML. The FNS cultures were subjected to nutlin-3 (15 and 30  $\mu$ M) for 24 and 48 h. As shown in **Figure 6A**, the cell viabilities decreased in a dose- and time-

## Proteomic profiling of facial nerve schwannomas

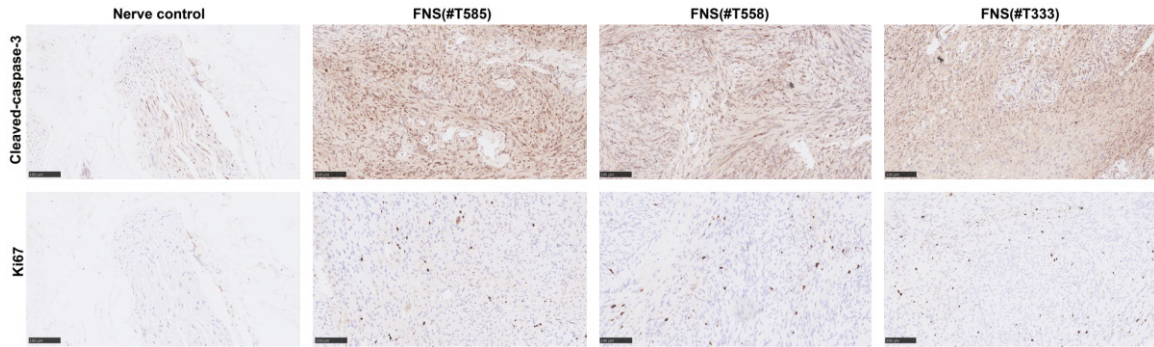


**Figure 5.** Expression of cleaved-Caspase 3 and Ki67 in FNS compared with normal nerve control by Immunohistochemistry. Significantly higher expression of cleaved-Caspase 3 (upper part) is noted in FNS (tumours #T585, #T558, and #T333) than the great auricular nerve control. No significant expression (<5% immunostaining) of Ki-67 (lower part) was detected in both tumor and nerve control. Scale bar =100  $\mu$ m.

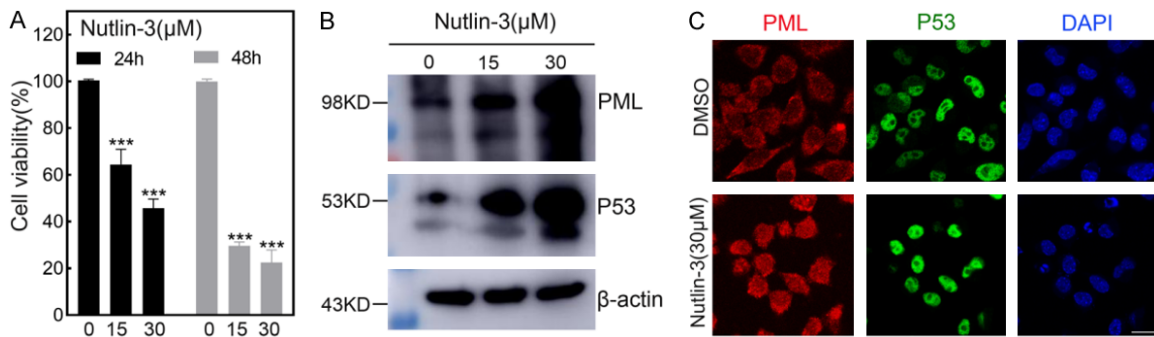


**Figure 6.** Inhibitory effects of nutlin-3 on the proliferation of facial nerve schwannoma cells (FSC) in vitro. A. FSC were treated with different doses of nutlin-3 for 24 and 48 h. CCK-8 assays showed that the cell viabilities decreased in a dose- and time-dependent manner in response to nutlin-3. Data are represented as mean  $\pm$  SD. \* $P$ <0.05, \*\* $P$ <0.01 and \*\*\* $P$ =0.001 compared with controls. B. Western blotting showed the changes in the levels of PML and p53 in response to nutlin-3 at different doses for 24 h. P53 was induced by nutlin-3 treatment in a dose-dependent manner, and the induction occurred concomitantly with an increase in PML production. C. Immunofluorescence analysis shows no significant alterations in the subcellular localization of PML and p53 upon nutlin-3 treatment at 30  $\mu$ M for 24 h. Scale bar =25  $\mu$ m. Full-length gels are presented in [Figure S3](#).

dependent manner in response to nutlin-3. The viability of FSC ( $45.7 \pm 15.3\%$ ;  $P=0.001$ ) with nutlin-3 at 30  $\mu$ M was significantly decreased compared with that of DMSO-treated control cells on day 1. Western blotting showed that p53 was induced by nutlin-3 treatment in a dose-dependent manner, and the induction occurred concomitantly with an increase in PML production (**Figure 6B**). This observation was consistent with the notion that overexpression of PML/p53 may be one of the tumour suppressor mechanisms in FNS. In contrast to the large differences in p53 and PML levels upon nutlin-3 treatments, immunofluorescence analysis revealed no obvious changes in the subcellular localization of the two proteins (**Figure 6C**).

## Discussion

FNS represents one of the more difficult treatment paradigms in neurotology, and due to its low prevalence, there is a lack of molecular data concerning this disease. In contrast to the frequent occurrence of truncating mutations of *NF2* in vestibular schwannomas, none of the FNS samples in our study showed such mutations. The lack of *NF2* mutations did not correlate with the deficiency of merlin protein in the tumour samples analyzed. These cases may show loss of heterozygosity (LOH) of chromosome 22 or large deletions involving the *NF2* gene that was not detectable by direct sequencing. This notion agreed with a previous study

showing the loss of 22q in an FNS sample [2]. Agnihotri and colleagues [4] have recently identified mutations in additional genes not previously reported in sporadic schwannomas (64 vestibular and 62 spinal schwannomas), including *ARID1*, *DDR1*, *TAB3*, *ALPK2*, *CAST* and *TSC1/2*. Therefore, it cannot be excluded that an initial mutation in other genes exists and is somehow implicated in regulating the expression or stability of merlin, thus leading to the loss of the protein.

It is widely accepted that the loss of function of merlin is central to the pathogenesis of schwannomas [35]. The inactivation of merlin was shown to trigger the activation of signaling pathways contributing to schwannoma proliferation, including Ras, Rac, mitogen-activated protein kinase, p21-activated kinase, and various receptor tyrosine kinases [36]. However, significant apoptotic expression has been described in the skin and subcutaneous schwannomas [30]. A high apoptotic index was found to correlate with a high proliferation rate, and was observed after radiotherapy for recurrent schwannomas [29, 31]. The current study revealed the first comprehensive proteomic profiling of FNS. One of the most significant results was the aberrant expression of PML-p53 partner proteins in FNS. The accumulation of yes-associated protein (YAP), a major effector of the Hippo pathway, triggers the formation of a PML-YAP complex, whose activity is associated with the pro-apoptotic functions of p53 [37]. Thus, YAP appears to bridge the tumour-suppressor activities of p53 and PML. Indeed, in several models, the loss of merlin expression results in the nuclear accumulation of YAP [38, 39]. Considering these findings, it is likely that deregulation of PML-p53 may occur as part of the protective cellular mechanisms in response to the proliferation signal mediated by the loss of merlin expression in FNS. Up-regulation of the apoptotic markers, PML and p53, in FNS were consistent with the observation that the *in vitro* proliferation of tumour cells was significantly suppressed compared with that of Schwann cells.

The pro-apoptotic roles of PML-p53, partner proteins positively regulating each other to trigger apoptosis, highlight the therapeutic potential of the induction of both proteins in the treatment of FNS. Therefore, using pre-existing drugs (e.g., nutlins) that target p53, it may be

possible to further induce coordinated expression of PML and p53 to suppress the growth of FNS. Nutlin-3 has shown considerable promise in preclinical studies against cancers [40]. Recently, we have indicated that p53 activation by nutlin-3 can lead to an impressive regression in schwannoma cell lines RT4 and HEI-193, and murine xenograft models of both cell lines [23]. The present study suggested that nutlin-3 exerted inhibitory effects on FNS cultures by promoting the protein levels of p53 and PML in a dose- and time-dependent manner, although the detailed contribution of PML relative to p53 during the treatment remains unknown.

Our study has some limitations. First, the study involved only 12 cases of sporadic FNS, because of the low prevalence of the tumour. Increased sample sizes are needed for future analysis. We chose the great auricular nerves (GANs) for proteomics and western blotting analyses because the normal facial nerves are difficult to obtain. Nevertheless, schwannomas and diseases of the GANs are exceptionally rare, making it an excellent source of healthy Schwann cells. Second, we used Sanger sequencing as the method for detecting mutations. However, this method only detects point mutations or small deletion/insertions. To fully reveal the mutational status of the *NF2* gene in FNS, a future study should involve a combination of approaches including direct sequencing, multiplex ligation-dependent probe amplification, and LOH analysis. liquid chromatography-tandem mass spectrometry (LC-MS/MS)-based methodology is not sensitive enough to detect small and highly charged peptides, hydrophobic membrane proteins, and lowly expressed proteins [41, 42]. The merlin protein is a good example, because changes in merlin expression levels cannot be detected by LC-MS/MS [11]. Because LC-MS/MS and capillary electrophoresis-tandem mass spectrometry are highly complementary techniques in identifying peptide sequences, employing both techniques in future investigations might result in substantially increased proteomic information. Finally, the primary cultures of FNS were only grown for a limited number of cell passages, making it difficult to carry out in-depth investigations-for example, overexpression/knockdown experiments to confirm the regulation of PML in the proliferation and apoptosis of FNS cultures. Despite these limitations, the current study



may present a potential treatment target for FNS.

### Acknowledgements

This work was supported by the National Natural Science Foundation of China (Grant No. 81800898 to Hongsai Chen, Grant No. 8167-0919 and 81870713 to Zhaoyan Wang, and Grant No. 81970872 to Hao Wu), and Shanghai Key Laboratory of Translational Medicine on Ear and Nose Diseases (14DZ2260300).

### Disclosure of conflict of interest

None.

**Address correspondence to:** Zhaoyan Wang and Hao Wu, Department of Otolaryngology Head & Neck Surgery, The Ninth People's Hospital, School of Medicine, Shanghai Jiao Tong University, No. 639, Zhi-Zao-Ju Road, Shanghai 200011, China. Tel: +86-021-25078891; Fax: +86-021-65156489; E-mail: wzyent@126.com (ZYW); wuhao622@sina.cn (HW)

### References

- [1] Quesnel AM and Santos F. Evaluation and management of facial nerve schwannoma. *Otolaryngol Clin North Am* 2018; 51: 1179-1192.
- [2] Fenton JE, Morrin MM, Smail M, Sterkers O and Sterkers JM. Bilateral facial nerve schwannomas. *Eur Arch Otorhinolaryngol* 1999; 256: 133-135.
- [3] van den Munckhof P, Christiaans I, Kenter SB, Baas F and Hulsebos TJ. Germline SMARCB1 mutation predisposes to multiple meningiomas and schwannomas with preferential location of cranial meningiomas at the falx cerebri. *Neurogenetics* 2012; 13: 1-7.
- [4] Agnihotri S, Jalali S, Wilson MR, Danesh A, Li M, Klironomos G, Krieger JR, Mansouri A, Khan O, Mamatjan Y, Landon-Brace N, Tung T, Dowar M, Li T, Bruce JP, Burrell KE, Tonge PD, Alamsahebpour A, Krischek B, Agarwalla PK, Bi WL, Dunn IF, Beroukhim R, Fehlings MG, Brill V, Pagnotta SM, Iavarone A, Pugh TJ, Aldape KD and Zadeh G. The genomic landscape of schwannoma. *Nat Genet* 2016; 48: 1339-1348.
- [5] Hadfield KD, Smith MJ, Urquhart JE, Wallace AJ, Bowers NL, King AT, Rutherford SA, Trump D, Newman WG and Evans DG. Rates of loss of heterozygosity and mitotic recombination in NF2 schwannomas, sporadic vestibular schwannomas and schwannomatosis schwannomas. *Oncogene* 2010; 29: 6216-6221.
- [6] Kehrer-Sawatzki H, Farschtschi S, Mautner VF and Cooper DN. The molecular pathogenesis of schwannomatosis, a paradigm for the co-involvement of multiple tumour suppressor genes in tumorigenesis. *Hum Genet* 2017; 136: 129-148.
- [7] Ikeda T, Hashimoto S, Fukushige S, Ohmori H and Horii A. Comparative genomic hybridization and mutation analyses of sporadic schwannomas. *J Neurooncol* 2005; 72: 225-230.
- [8] Zhou L and Hanemann CO. Merlin, a multi-suppressor from cell membrane to the nucleus. *FEBS Lett* 2012; 586: 1403-1408.
- [9] Chen H, Xue L, Wang H, Wang Z and Wu H. Differential NF2 gene status in sporadic vestibular schwannomas and its prognostic impact on tumour growth patterns. *Sci Rep* 2017; 7: 5470.
- [10] Ahmad Z, Brown CM, Patel AK, Ryan AF, Ongkeko R and Doherty JK. Merlin knockdown in human Schwann cells: clues to vestibular schwannoma tumorigenesis. *Otol Neurotol* 2010; 31: 460-466.
- [11] Bassiri K, Ferluga S, Sharma V, Syed N, Adams CL, Lasonder E and Hanemann CO. Global proteome and phospho-proteome analysis of merlin-deficient meningioma and schwannoma identifies PDLIM2 as a novel therapeutic target. *EBioMedicine* 2017; 16: 76-86.
- [12] Dilwali S, Patel PB, Roberts DS, Basinsky GM, Harris GJ, Emerick KS and Stankovic KM. Primary culture of human Schwann and schwannoma cells: improved and simplified protocol. *Hear Res* 2014; 315: 25-33.
- [13] Li X, Chen H, Xue L, Pang X, Zhang X, Zhu Z, Zhu W, Wang Z and Wu H. p53 performs an essential role in mediating the oncogenic stimulus triggered by loss of expression of neurofibromatosis type 2 during in vitro tumor progression. *Oncol Lett* 2017; 14: 2223-2231.
- [14] Graf SA, Hept MV, Wessely A, Krebs S, Kammerbauer C, Hornig E, Strieder A, Blum H, Bosserhoff AK and Berking C. The myelin protein PMP2 is regulated by SOX10 and drives melanoma cell invasion. *Pigment Cell Melanoma Res* 2019; 32: 424-434.
- [15] Torres-Martín M, Lassaletta L, de Campos JM, Isla A, Pinto GR, Burbano RR, Melendez B, Castresana JS and Rey JA. Genome-wide methylation analysis in vestibular schwannomas shows putative mechanisms of gene expression modulation and global hypomethylation at the HOX gene cluster. *Genes Chromosomes Cancer* 2015; 54: 197-209.
- [16] Kakizuka A, Miller WH Jr, Umehono K, Warrell RP Jr, Frankel SR, Murty VV, Dmitrovsky E and Evans RM. Chromosomal translocation t(15;17) in human acute promyelocytic leukemia fuses RAR alpha with a novel putative



## Proteomic profiling of facial nerve schwannomas

- transcription factor, PML. *Cell* 1991; 66: 663-674.
- [17] Gurrieri C, Capodiecì P, Bernardi R, Scaglioni PP, Nafa K, Rush LJ, Verbel DA, Cordon-Cardo C and Pandolfi PP. Loss of the tumor suppressor PML in human cancers of multiple histologic origins. *J Natl Cancer Inst* 2004; 96: 269-279.
- [18] Koken MH, Linares-Cruz G, Quignon F, Viron A, Chelbi-Alix MK, Sobczak-Thépot J, Juhlin L, Degos L, Calvo F and de Thé H. The PML growth-suppressor has an altered expression in human oncogenesis. *Oncogene* 1995; 10: 1315-1324.
- [19] Zhu Z, Khan MA, Weiler M, Blaes J, Jestaedt L, Geibert M, Zou P, Gronych J, Bernhardt O, Korshunov A, Bugner V, Lichter P, Radlwimmer B, Heiland S, Bendszus M, Wick W and Liu HK. Targeting self-renewal in high-grade brain tumors leads to loss of brain tumor stem cells and prolonged survival. *Cell Stem Cell* 2014; 15: 185-198.
- [20] Sherman L, Jacoby LB, Lampe J, Pelton P, Aguzzi A, Herrlich P and Ponta H. CD44 expression is aberrant in benign Schwann cell tumors possessing mutations in the neurofibromatosis type 2, but not type 1, gene. *Cancer Res* 1997; 57: 4889-4897.
- [21] Utermark T, Kaempchen K and Hanemann CO. Pathological adhesion of primary human schwannoma cells is dependent on altered expression of integrins. *Brain Pathol* 2003; 13: 352-363.
- [22] Flaiz C, Ammoun S, Biebl A and Hanemann CO. Altered adhesive structures and their relation to RhoGTPase activation in merlin-deficient Schwannoma. *Brain Pathol* 2009; 19: 27-38.
- [23] Chen H, Xue L, Huang H, Wang H, Zhang X, Zhu W, Wang Z, Wang Z and Wu H. Synergistic effect of Nutlin-3 combined with MG-132 on schwannoma cells through restoration of merlin and p53 tumour suppressors. *EBioMedicine* 2018; 36: 252-265.
- [24] Bernardi R, Scaglioni PP, Bergmann S, Horn HF, Vousden KH and Pandolfi PP. PML regulates p53 stability by sequestering Mdm2 to the nucleolus. *Nat Cell Biol* 2004; 6: 665-672.
- [25] de Stanchina E, Querido E, Narita M, Davuluri RV, Pandolfi PP, Ferbeyre G and Lowe SW. PML is a direct p53 target that modulates p53 effector functions. *Mol Cell* 2004; 13: 523-535.
- [26] Chang HJ, Yoo BC, Kim SW, Lee BL and Kim WH. Significance of PML and p53 protein as molecular prognostic markers of gallbladder carcinomas. *Pathol Oncol Res* 2007; 13: 326-335.
- [27] Gamell C, Jan Paul P, Haupt Y and Haupt S. PML tumour suppression and beyond: therapeutic implications. *FEBS Lett* 2014; 588: 2653-2662.
- [28] Shen TH, Lin HK, Scaglioni PP, Yung TM and Pandolfi PP. The mechanisms of PML-nuclear body formation. *Mol Cell* 2006; 24: 331-339.
- [29] Abe M, Kawase T, Urano M, Mizoguchi Y, Kuroda M, Kasahara M, Suzuki H and Kanno T. Analyses of proliferative potential in schwannomas. *Brain Tumor Pathol* 2000; 17: 35-40.
- [30] Martin De Las Mulas J, Millan Y, Ruiz-Villamor E, Bautista MJ, Rollon E and Espinosa De Los Monteros A. Apoptosis and mitosis in tumours of the skin and subcutaneous tissues of the dog. *Res Vet Sci* 1999; 66: 139-146.
- [31] Lee F, Linthicum F Jr and Hung G. Proliferation potential in recurrent acoustic schwannoma following gamma knife radiosurgery versus microsurgery. *Laryngoscope* 2002; 112: 948-950.
- [32] Seo JH, Park KH, Jeon EJ, Chang KH, Lee H, Lee W and Park YS. Proteomic analysis of vestibular schwannoma: conflicting role of apoptosis on the pathophysiology of sporadic vestibular schwannoma. *Otol Neurotol* 2015; 36: 714-719.
- [33] Hakin-Smith V, Battersby RD, Maltby EL, Timperley WR and Royds JA. Elevated p53 expression in benign meningiomas protects against recurrence and may be indicative of senescence. *Neuropathol Appl Neurobiol* 2001; 27: 40-49.
- [34] Arva NC, Talbott KE, Okoro DR, Brekman A, Qiu WG and Bargonetti J. Disruption of the p53-Mdm2 complex by Nutlin-3 reveals different cancer cell phenotypes. *Ethn Dis* 2008; 18 Suppl 2: S2-1-8.
- [35] Hilton DA and Hanemann CO. Schwannomas and their pathogenesis. *Brain Pathol* 2014; 24: 205-220.
- [36] Stamenkovic I and Yu Q. Merlin, a "magic" linker between extracellular cues and intracellular signaling pathways that regulate cell motility, proliferation, and survival. *Curr Protein Pept Sci* 2010; 11: 471-484.
- [37] Lapi E, Di Agostino S, Donzelli S, Gal H, Domany E, Rechavi G, Pandolfi PP, Givol D, Strano S, Lu X and Blandino G. PML, YAP, and p73 are components of a proapoptotic autoregulatory feedback loop. *Mol Cell* 2008; 32: 803-814.
- [38] Striedinger K, VandenBerg SR, Baia GS, McDermott MW, Gutmann DH and Lal A. The neurofibromatosis 2 tumor suppressor gene product, merlin, regulates human meningioma cell growth by signaling through YAP. *Neoplasia* 2008; 10: 1204-1212.
- [39] Furukawa KT, Yamashita K, Sakurai N and Ohno S. The epithelial circumferential actin belt regulates YAP/TAZ through nucleocytoplasmic shuttling of Merlin. *Cell Rep* 2017; 20: 1435-1447.

## Proteomic profiling of facial nerve schwannomas

- [40] Tovar C, Rosinski J, Filipovic Z, Higgins B, Kolinsky K, Hilton H, Zhao X, Vu BT, Qing W, Packman K, Myklebost O, Heimbrook DC and Vassilev LT. Small-molecule MDM2 antagonists reveal aberrant p53 signaling in cancer: implications for therapy. *Proc Natl Acad Sci U S A* 2006; 103: 1888-1893.
- [41] BassoM Giraud S, Corpillo D, Bergamasco B, Lopiano L and Fasano M. Proteome analysis of human substantia nigra in Parkinson's disease. *Proteomics* 2004; 4: 3943-3952.
- [42] Klein J, Papadopoulos T, Mischak H and Mullen W. Comparison of CE-MS/MS and LC-MS/MS sequencing demonstrates significant complementarity in natural peptide identification in human urine. *Electrophoresis* 2014; 35: 1060-1064.

## Proteomic profiling of facial nerve schwannomas

**Table S1.** Genetic information of patients with sporadic facial nerve schwannoma (FNS) and vestibular schwannomas (VSs) as controls

Case	Diagnosis	<i>NF2</i> gene point mutation				<i>LZTR1</i> gene point mutation				<i>SMARCB1</i> gene point mutation			
		Exon	Sequence alteration	Codon	Consequence	Exon	Sequence alteration	Codon	Consequence	Exon	Sequence alteration	Codon	Consequence
T333	FNS	None	None	None	None	None	None	None	None	None	None	None	None
T405	FNS	None	None	None	None	None	None	None	None	None	None	None	None
T475	FNS	None	None	None	None	E02	c.210G>A	p.K70K	Synonymous	E07	c.897G>A	p.S299S	Synonymous
						E18	c.2208C>T	p.P736P	Synonymous				
T562	FNS	None	None	None	None	E15	c.1683C>T	p.R561R	Synonymous	None	None	None	None
T558	FNS	None	None	None	None	E15	c.1683C>T	p.R561R	Synonymous	None	None	None	None
T585	FNS	None	None	None	None	E02	c.210G>A	p.K70K	Synonymous	None	None	None	None
						E15	c.1683C>T	p.R561R	Synonymous				
T611	FNS	None	None	None	None	None	None	None	None	None	None	None	None
T274	FNS	None	None	None	None	None	None	None	None	None	None	None	None
T278	FNS	None	None	None	None	None	None	None	None	None	None	None	None
T464	FNS	None	None	None	None	None	None	None	None	None	None	None	None
T474	FNS	None	None	None	None	None	None	None	None	None	None	None	None
T528	FNS	None	None	None	None	E02	c.210G>A	p.K70K	Synonymous	None	None	None	None
T543	VSs	None	None	None	None	None	None	None	None	None	None	None	None
T554	VSs	E13	c.1437delC	p479pfs*6	Frameshift	None	None	None	None	None	None	None	None
T561	VSs	None	None	None	None	E02	c.210G>A	p.K70K	Synonymous	None	None	None	None
T563	VSs	E02	c.169C>T	p.R57-	Nonsense	None	None	None	None	None	None	None	None

## Proteomic profiling of facial nerve schwannomas

**Table S3.** Gene Ontology (GO) analyses of the up- and down-regulated proteins

Category	Term	Count	
Up-regulated proteins			
BP	Cellular process	32	
	Response to stimulus	22	
	localization	21	
	Macromolecule localization	16	
	Response to organic substance	14	
	Response to stress	13	
	Cellular localization	13	
	Protein localization	13	
	Anatomical structure development	12	
	Developmental process	12	
	CC	cytoplasm	30
		intracellular	28
		Intracellular membrane bounded organelle	24
		Membrane bounded organelle	23
Intracellular organelle		22	
Cell periphery		22	
Plasma membrane		21	
vesicle		20	
membrane		19	
Extracellular region		17	
MF		Peptide binding	35
	Protein binding	33	
	Amide binding	28	
	Identical protein binding	15	
	RNA binding	10	
	Enzyme binding	8	
	Protein containing complex binding	7	
	Cytoskeletal protein_binding	7	
	Actin binding	7	
	Structural molecule activity	6	
	Down-regulated proteins		
BP	Cellular process	38	
	Anatomical structure development	25	
	Developmental process	25	
	Response to stimulus	24	
	System development	24	
	Multicellular organism development	24	
	localization	20	
	Cell differentiation	17	
	Animal organ development	16	
	Response to stress	13	
	CC	intracellular	41
		Intracellular organelle	40
		Membrane bounded organelle	39
		cytoplasm	35
membrane		32	



## Proteomic profiling of facial nerve schwannomas

	Extracellular region	28
	Extracellular vesicle	28
	Extracellular exosome vesicle	27
	Extracellular space	26
MF	Amide binding	35
	Protein binding	30
	Peptide binding	28
	Structural molecule activity	13
	Identical protein binding	12
	Protein containing complex binding	9
	Enzyme binding	8
	Protein dimerization activity	7
	Protein domain specific binding	7
	Cytoskeletal protein binding	6

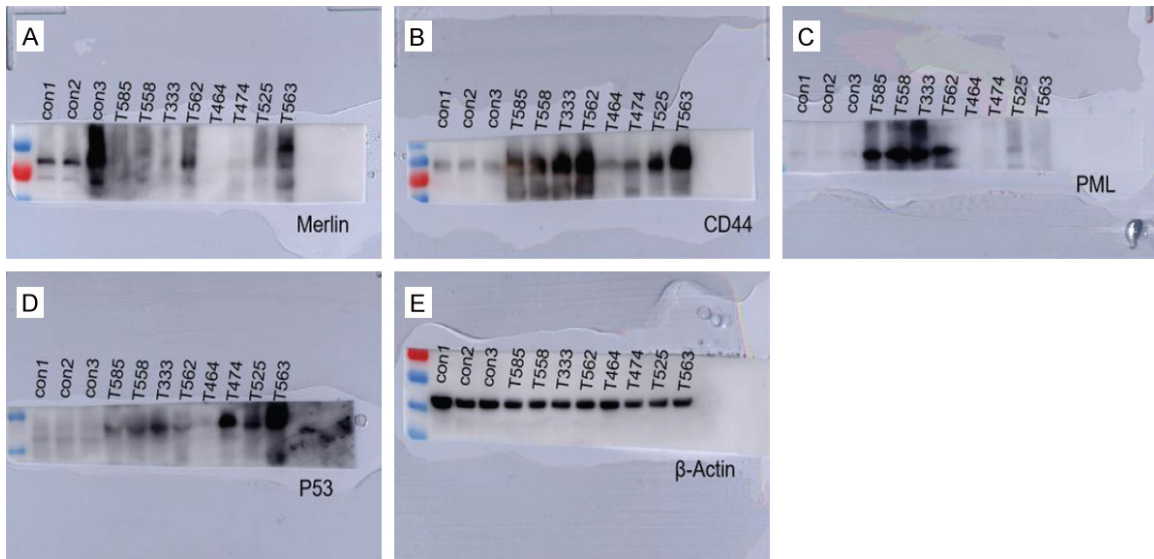


**Figure S1.** Original WB data for **Figure 3**. A. Full-length gel for Merlin. B. Full-length gel for CD44. C. Full-length gel for PML. D. Full-length gel for P53. E. Full-length gel for  $\beta$ -actin.

## Proteomic profiling of facial nerve schwannomas

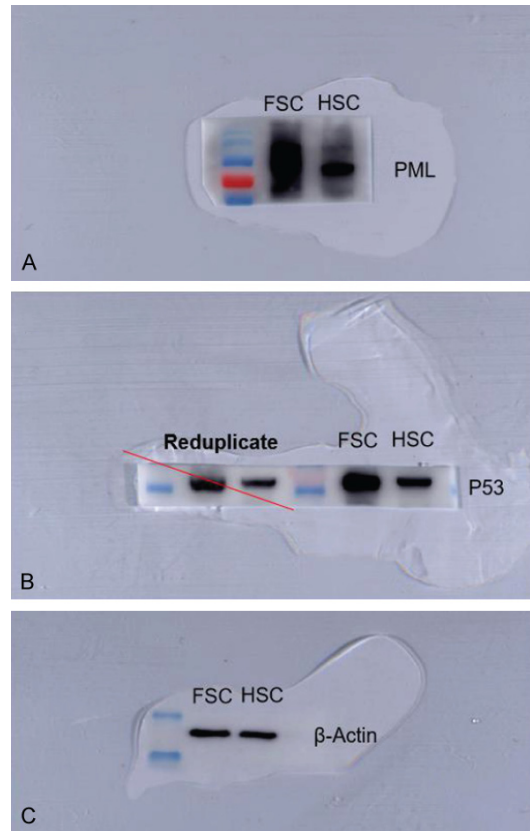


**Figure S2.** Original WB data for **Figure 4**. A. Full-length gel for PML. B. Full-length gel for P53. C. Full-length gel for  $\beta$ -actin.

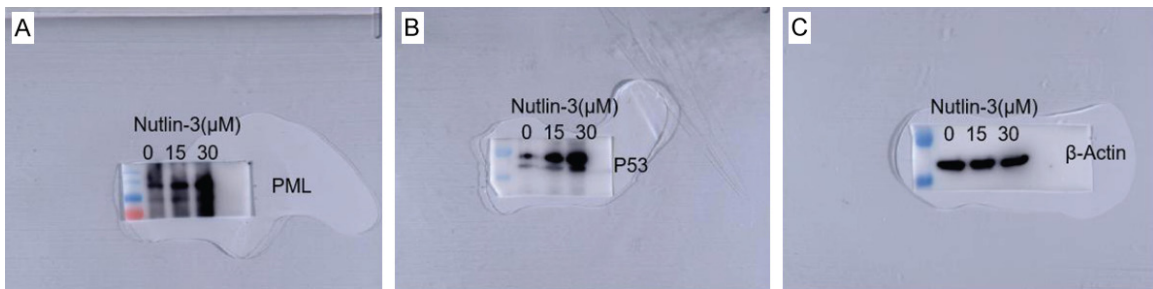


**Figure S3.** Original WB data for **Figure 6**. A. Full-length gel for PML. B. Full-length gel for P53. C. Full-length gel for  $\beta$ -actin.